JOURNAL OF GEOPHYSICAL RESEARCH, VOL. 112, D11112, doi:10.1029/2006JD007507, 2007

A climatological study of evapotranspiration and moisture stress across the continental United States based on thermal remote sensing: 2. Surface moisture climatology

Martha C. Anderson,[1] John M. Norman,[2] John R. Mecikalski,[3] Jason A. Otkin,[4] and William P. Kustas[1]

Received 12 May 2006; revised 26 October 2006; accepted 29 January 2007; published 9 June 2007.

[1] Robust satellite-derived moisture stress indices will be beneficial to operational drought monitoring, both in the United States and globally. Using thermal infrared imagery from the Geostationary Operational Environmental Satellites (GOES) and vegetation information from the Moderate Resolution Imaging Spectrometer (MODIS), a fully automated inverse model of Atmosphere-Land Exchange (ALEXI) has been used to model daily evapotranspiration and surface moisture stress over a 10-km resolution grid covering the continental United States. Examining monthly clear-sky composites for April–October 2002–2004, the ALEXI evaporative stress index (ESI) shows good spatial and temporal correlation with the Palmer drought index but at considerably higher spatial resolution. The ESI also compares well to anomalies in monthly precipitation fields, demonstrating that surface moisture has an identifiable thermal signature that can be detected from space, even under dense vegetation cover. Simple empirical thermal drought indices like the vegetation health index do not account for important forcings on surface temperature, such as available energy and atmospheric conditions, and can therefore generate spurious drought detections under certain circumstances. Surface energy balance inherently incorporates these forcings, constraining ESI response in both energy- and water-limited situations. The surface flux modeling techniques described here have demonstrated skill in identifying areas subject to soil moisture stress on the basis of the thermal land surface signature, without requiring information regarding antecedent rainfall. ALEXI therefore may have potential for operational drought monitoring in countries lacking well-established precipitation measurement networks.

Citation: Anderson, M. C., J. M. Norman, J. R. Mecikalski, J. A. Otkin, and W. P. Kustas (2007), A climatological study of evapotranspiration and moisture stress across the continental United States based on thermal remote sensing: 2. Surface moisture climatology, *J. Geophys. Res.*, *112*, D11112, doi:10.1029/2006JD007507.

1. Introduction

[2] Reliable methods for mapping evapotranspiration (ET) and land surface moisture status from space will greatly enhance our ability to manage our Earth's water resources and to respond quickly and effectively to localized reductions in food production due to drought. In the western United States, for example, remotely sensed ET maps are routinely used to estimate lower limits on agricultural and urban consumptive water use, and evaporative losses from irrigated fields, reservoirs and riparian zones [*Bastiaanssen et al.*, 2005; *Tasumi et al.*, 2005], and in the negotiation and monitoring of water rights [*Allen et al.*, 2005]. Satellite-based drought indices are being used operationally to supplement data from ground-based weather and precipitation networks to assess drought conditions in the United States [*Svoboda et al.*, 2002]. For maximized utility, moisture index products feeding operational monitoring programs should be based on stable data sources with long-term availability rather than on instruments on research platforms, which may have limited lifetime.

[3] Because land-surface temperature (LST) is strongly modulated by evaporation, remote sensing data in the thermal infrared (TIR) bands carry valuable information regarding surface moisture availability. A companion paper [*Anderson et al.*, 2007] (hereinafter referred to as A1) describes a regional surface energy balance modeling system—the Atmosphere-Land Exchange Inverse (ALEXI) model—that has potential for routine, long-term mapping of ET and soil moisture stress. ALEXI is driven primarily by

[1]Hydrology and Remote Sensing Laboratory, Agricultural Research Service, U.S. Department of Agriculture, Beltsville, Maryland, USA.
[2]Department of Soil Science, University of Wisconsin-Madison, Madison, Wisconsin, USA.
[3]National Space Science and Technology Center, University of Alabama in Huntsville, Huntsville, Alabama, USA.
[4]Cooperative Institute for Meteorological Satellite Studies, University of Wisconsin-Madison, Madison, Wisconsin, USA.

0148-0227/07/2006JD007507$09.00

TIR imagery from the Geostationary Operational Environmental Satellites (GOES), an excellent (albeit underutilized) data source for routine land surface monitoring. GOES has high temporal frequency (15 min) and continental-scale coverage, and its operational status, integral to national weather forecasting applications, means a long history of archived data and a good likelihood of continuation. A1 discuss techniques for extrapolating instantaneous ALEXI flux predictions made under cloud-free conditions to full hourly and daily coverage in every cell of the model domain. These techniques use the ratio (f_{PET}) of actual to potential ET (PET) to infer subsurface soil moisture content on clear days, and invert the ET-soil moisture relationships to predict moisture fluxes under cloudy conditions when satellite-based surface temperature data are unavailable. ET predictions and extrapolations were compared by A1 to watershed-scale distributed flux observations collected during a field experiment in central Iowa in 2002.

[4] Using thermal band imagery from GOES and vegetation cover information from the Moderate Resolution Imaging Spectrometer (MODIS), the ALEXI algorithm has been executed over a 10-km resolution grid covering the continental United States for April–October of 2002–2004, focusing on periods when most of the domain is free of snow. In this paper we look more qualitatively at interannual and intra-annual temporal patterns in maps of ET and f_{PET} generated with the ALEXI algorithm over this 3-year interval. Here, f_{PET} is interpreted as a signature of soil moisture availability and is expressed as an evaporative stress index (ESI).

[5] Regional-scale land surface flux and drought models are difficult to validate rigorously, given current scarcity in scale-appropriate validation data. Therefore patterns in the ESI are assessed in comparison with contemporaneous gridded precipitation data and with other standard meteorologically based indices of drought and surface moisture stress to determine whether thermal remote sensing, as interpreted by ALEXI, provides useful information regarding drought conditions at continental scales.

2. TIR-Based Drought Indices

[6] Quantitative measures of drought are typically associated with a specific temporal scale, dependent on the hydrologic impact of interest and its nominal timescale for recovery [*Dracup et al.*, 1980; *Wilhite and Glantz*, 1985]. Meteorological drought describes a deficit in precipitation relative to the long-term local average and can be relieved rapidly with a good rainfall event. Agricultural drought, which impacts crop yield, is related to moisture deficiencies in the root zone and tracks time constants associated with plant water uptake and soil profile rewetting. Hydrologic drought affects streamflow, groundwater tables and reservoir levels, and occurs and recovers over much longer timescales of months to years. A set of specific criteria for quantitatively evaluating the utility of drought indices was proposed by *Keyantash and Dracup* [2002], including measures of robustness and transparency in terms of physical meaning.

[7] Current algorithms for computing meteorological, agricultural and hydrologic drought indices involve various levels of empiricism and complexity and utilize many different sources of input data, some based on ground observations and others derived through remote sensing. The standard metrics, such as the Palmer drought severity index (PDSI), generally require spatially distributed estimates of precipitation and soil water holding capacity. These data are not currently available with good accuracy at the continental scale and limit the spatial resolution of the output product. The advantage of a drought metric based on remote sensing is that ground-based data needs are limited, thereby improving spatial detail and portability to areas without extensive weather and precipitation networks. Remote sensing approaches to drought mapping provide a snapshot of current land surface conditions, and are therefore better measures of meteorological and agricultural drought than long-term hydrologic drought, although the indices can be accumulated in time to track persistent moisture deficits.

[8] *Moran* [2003] reviews applications of TIR remote sensing data in assessing water stress in plant ecosystems. *Idso et al.* [1981] and *Jackson et al.* [1981] developed the crop water stress index (CWSI) on the basis of the ratio of actual to potential ET, as evaluated by applying the Penman-Monteith equation [*Monteith*, 1965] for full canopy cover. *Moran et al.* [1994] extended application to partial canopies by including information about vegetation cover amount derived from surface reflectance data, forming the water deficit index (WDI). Both the CWSI and WDI rely on measurements of the surface-to-air temperature difference, which reflects the degree of stress-induced stomatal closure and resulting decrease in transpiration from the vegetative canopy. While this gradient can be measured locally, it is difficult to assess with accuracy over regional scales due to the sparsity of shelter-level air temperature measurements and lack of cross calibration between the air and satellite-based TIR temperature sensors.

[9] Of current drought metrics derived solely from spaceborne data, the vegetation health index (VHI) [*Kogan*, 1997] has been widely accepted as an operational tool for global drought monitoring. The VHI is a weighted average of normalized satellite-derived surface temperature and normalized difference vegetation index (NDVI), scaled between representative maximum and minimum values found at each pixel over some period of record. The formulation of the VHI presupposes that temperature and NDVI are anticorrelated, with high-cover areas being cooler and deviations from this relationship interpreted as a signature of stress. *Karnieli et al.* [2006], however, demonstrate that when vegetation growth is energy limited, as in cooler climates or at higher elevations, surface temperature and NDVI can be directly correlated, causing spurious stress signals in the VHI. *Bayarjargal et al.* [2006] compared several satellite-derived drought indices on the basis of simple normalized combinations of temperature and/or vegetation index (VI). They found no consistent spatial coincidence between the indices over the desert and desert steppe regions of Mongolia, and limited correlation with meteorological indices such as the PDSI or ground observations of drought-affected areas.

[10] We suggest that a better approach to merging TIR/VI remote sensing data into a unified drought metric is within the context of a surface energy balance model, where these signatures can be evaluated in relationship to soil moisture status in a physically meaningful way. Energy balance determines the thermal state of an evaporating land surface under varying vegetation cover fraction, radiation load, and ambient climatic conditions. If important driving factors are neglected in the interpretation of TIR/VI data, the resulting index may not be a reliable tool for assessing drought conditions at continental or global scales.

3. Methods

3.1. ALEXI Model

[11] The ALEXI surface energy balance model was specifically designed to minimize the need for ancillary meteorological data while maintaining a physically realistic representation of land-atmosphere exchange over a wide range in vegetation cover conditions. ALEXI deduces the land surface energy balance from the morning rise in radiometric surface temperature, as measured from a geostationary platform between times t_1 and t_2 (1.5 and ~5.5 hours past local sunrise). Keying to a time differential temperature measure reduces model sensitivity to errors in sensor calibration and atmospheric correction. The two-source land surface component of ALEXI partitions net radiation (RN, W m^{-2}) into sensible heating (H, W m^{-2}), latent heating (λE; W m^{-2}, where E is evapotranspiration in mm s^{-1} or kg s^{-1} m^{-2} and λ is the latent heat of evaporation, J kg^{-1}), and soil heat conduction (G, W m^{-2}) fluxes associated with the soil and canopy components of the scene (subscript s and c, respectively):

$$RN = H + \lambda E + G$$
$$RN_S = H_S + \lambda E_S + G \quad (1)$$
$$RN_C = H_C + \lambda E_C$$

on the basis of the local vegetation cover fraction (f_c), estimated from satellite-derived vegetation index or leaf area index (LAI) products. A simple slab model of atmospheric boundary layer development provides energy closure over the time interval between t_1 and t_2. The full algorithm is described in detail by *Anderson et al.* [1997] and *Mecikalski et al.* [1999], with recent improvements and input data sources discussed by A1.

3.2. Evaporative Stress Index

[12] Spatial and temporal variations in instantaneous ET at the continental scale are primarily due to variability in moisture availability (antecedent precipitation), radiative forcing (cloud cover, sun angle), vegetation amount, and local atmospheric conditions such as air temperature, wind speed and vapor pressure deficit. Potential ET describes the evaporation rate expected when soil moisture is nonlimiting, ideally capturing response to all other forcing variables. To isolate effects due to spatially varying soil moisture availability, a simple evaporative stress index (ESI) can be developed from model flux estimates, given by 1 minus the ratio of actual to potential ET following the formulation of the CWSI and WDI. Using ALEXI, we can derive evaporative stress indices associated with the canopy (ESI_c), the soil surface (ESI_s), and the combined plant-soil system (ESI):

$$ESI_C = 1 - f_{PETc} = 1 - \frac{E_C}{PET_C}$$
$$ESI_S = 1 - f_{PETs} = 1 - \frac{E_S}{PET_S} \quad (2)$$
$$ESI = 1 - f_{PET} = 1 - \frac{E}{PET} = 1 - \frac{E_C + E_S}{PET_C + PET_S}$$

where E_C, E_S and E are the modeled actual ET fluxes (mm) from the canopy, soil and system, respectively, and PET_C, PET_S, PET are potential rates associated with these components (mm; see Appendix B of A1 for forms used in this study to estimate PET). These indices have a value of 0 when there is ample moisture/no stress, and a value of 1 when evapotranspiration has been cut off because of stress-induced stomatal closure and/or complete drying of the soil surface.

[13] A1 demonstrate that f_{PETs} and f_{PETc} are sensitive to moisture stress over different timescales. The soil surface responds quickly to moisture deficiencies, and therefore ESI_S should be a better measure of meteorological drought, while the canopy indices change at a slower rate and are more appropriate for tracking agricultural drought conditions. In general, this stress may incorporate more than just limiting soil moisture conditions. Low f_{PET} in vegetated areas may result from stomatal closure because of very high air temperature and/or vapor pressure deficit (VPD). Although the word "stress" is usually applied to vegetation growing on soil depleted in moisture, for consistency we can identify reductions in evaporation from potential evaporation for bare soil regions as "stress" because it indicates drying conditions. In this study, we do not distinguish between causes of stress and refer to ESI approaching 1 as "evaporative stress" for both vegetated and bare surfaces.

[14] Among the existing regional TIR-based drought indices, the ALEXI evaporative stress index is unique in that it has a clearly defined physical meaning in terms of the impact on evaporative fluxes from the soil and canopy. It therefore has additional utility in terms of direct assimilation into other types of simulation systems, such as numerical weather prediction and surface hydrology models. It also has the advantage of being quantitatively verifiable in comparison with ground measurements (see A1). Of the several characteristics identified by *Keyantash and Dracup* [2002] as useful in evaluating the overall utility of operational drought indices, the ESI fulfills the criteria of transparency, nondimensionality and comparability between regions with different climatic and biotic conditions. However, because of its reliance on remote sensing data, the historical period over which the index can be computed to establish climatologically normal conditions is limited in comparison with indices based on point temperature or precipitation records which extend back to the early 1900s. Even so, GOES imagery and ancillary data have been archived over many decades and "normals" could be defined if desired or necessary.

3.3. Composites and Anomalies

[15] Given its dependence on the availability of remotely sensed surface temperature data, the ALEXI model can only be executed under clear-sky conditions. This means that a significant portion of the full continental domain may not be modeled on any given day. A1 describe a procedure for extrapolating the instantaneous clear-sky flux predictions from ALEXI to full hourly and daily coverage, including both clear and cloudy conditions, which can then be integrated to longer timescales (monthly, annual, etc). Alternatively, clear-sky fluxes can be composited over multiday intervals to fill in a larger fraction of the model domain.

[16] In this assessment of model utility for drought detection, we focus on 28-day composites of clear-sky ET and moisture stress fields from ALEXI, computed as

$$\bar{v}(m,y,i,j) = \frac{1}{nc}\sum_{n=1}^{nc} v(n,y,i,j) \tag{3}$$

where $\bar{v}$ (m, y, i, j) is an ALEXI output variable for month m, year y, and i, j grid location, and v (n, y, i, j) is the value on day n. For clear-sky composites, the number of values included in the average (nc) (i.e., the number of days during the compositing interval that pixel i, j was clear) will vary across the domain because of variations in persistence of cloud cover during month m. By filling the continental grids through compositing rather than extrapolation, we simplify interannual flux comparisons by reducing variability due to cloud effects on net radiation, and we isolate signatures from the clear-sky ALEXI algorithm from errors inherent in the extrapolation technique. Furthermore, clouds tend to relieve vegetation stress. The strongest signal of depleted soil moisture conditions in terms of elevated canopy temperature will be observed under clear-sky conditions.

[17] To highlight differences in moisture conditions between years, and to improve comparability with climatological indices like the Palmer drought index, stress index maps will be presented as anomalies in monthly composited values with respect to multiyear average fields determined over the period of record consisting of ny years:

$$\Delta\bar{v}(m,y,i,j) = \bar{v}(m,y,i,j) - \frac{1}{ny}\sum_{y=1}^{ny}\bar{v}(m,y,i,j). \tag{4}$$

[18] Analyses and comparability will improve as more years of model runs are accumulated; at present some spatial artifacts can be associated with the relatively short period of analysis (which is not truly representative of a long-term climatological mean).

3.4. Comparison Drought Metrics

[19] The Palmer Drought Indices [*Palmer*, 1965, 1968] have historically been the most commonly referenced measures of drought in the United States, although their functional deficiencies are well known. Given time series measurements of daily precipitation and air temperature, a simple two-layer soil model is used to estimate ET, soil moisture storage, recharge, and surface runoff. The Palmer family consists of three primary indices, each with a characteristic timescale. The Palmer moisture anomaly index (Z index) represents the departure of modeled soil moisture from the climatic mean for each month, independent of antecedent conditions. Longer-term drought indices are then developed from the Z index: the Palmer drought severity index (PDSI; a measure of meteorological drought) and the Palmer hydrologic drought severity index (PHDSI) result from an analysis of a monthly Z index time series with increasing stringent thresholds for determining when drought conditions have been alleviated. Of these, the Z index is most comparable with the ALEXI stress index, which samples instantaneous surface conditions, although moisture deficiencies from the previous month may be integrated in terms of their effects on current evaporative fluxes.

[20] *Heim* [2002] reviews the limitations of the Palmer Indices. The algorithms used to compute the index values are complex and opaque, and drought severity thresholds are somewhat arbitrary. The core model neglects the effect of seasonal changes in vegetation cover, snowmelt, and frozen soil on water budget partitioning [*Alley*, 1984]. Index values are not strictly comparable between seasons and climatic regions across the United States, complicating interpretation of the PDSI at the continental scale [*Alley*, 1984; *Guttman*, 1997; *Guttman et al.*, 1992]. The indices are also highly sensitive to choice of calibration coefficients and soil available water capacity [*Karl*, 1983, 1986].

[21] ALEXI stress index patterns will also be compared directly with anomalies in precipitation, determined over an identical period of record. Here we use daily gridded precipitation data derived from objective analyses of ground-based rainfall measurements (~5000 stations per day), performed by the Climate Prediction Center at a resolution of 0.25° × 0.25° http://www.cpc.ncep.noaa.gov/products/precip/realtime/GIS/USMEX/USMEX-precip.shtml). These precipitation data are used for comparison purposes only—the ALEXI model does not use precipitation as an input.

[22] The Drought Monitor [*Svoboda et al.*, 2002] (see also http://drought.unl.edu/dm) represents an effort to synthesize features present in multiple drought indices (including the PDSI and VHI), along with anecdotal evidence of moisture conditions relayed by experts in the field. It is a joint effort involving several federal agencies and academic institutions, and assessments are posted weekly in the form of low-resolution maps accompanied by a narrative description of regional conditions. Drought Monitor reports will be used to assess reliability of features in the ESI and other moisture status indices.

4. Climatological Results

4.1. Period of Record

[23] The ALEXI model was run daily during the months of April–September 2002–2004. This seasonal interval was selected in order to encompass most of crop growing cycle, while excluding periods of pervasive snow cover. Currently, the GOES-based insolation product used to constrain net radiation does not discriminate between snow cover and clouds [*Otkin et al.*, 2005]. Model input fields to ALEXI were developed as described by A1, using surface radiometric data from GOES and vegetation cover fraction

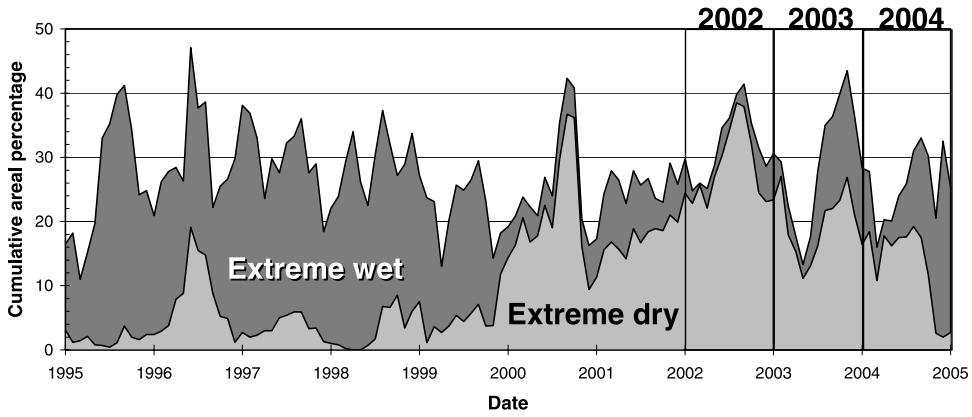

Figure 1. Cumulative areal percentage of the continental United States experiencing extreme dry conditions for 1995–2005, as predicted by the palmer drought index.

derived from the MODIS MOD15A LAI product [*Myneni et al.*, 2002].

[24] The 3 years encompassed in this climatological survey exhibit significant interannual variability in terms of nationwide drought conditions. Figure 1 represents monthly variations in percentage area of the United States experiencing extreme severe dry and wet conditions from 1996 to 2005, as quantified by the PDSI (National Climatic Data Center (NCDC)). In summary:

[25] 1. A combination of hot and dry conditions in 2002 created the worst extreme severe drought conditions that the United States has experienced during the last 40 years, peaking near 40% coverage in July and focused particularly in the Southwest, and spreading into the Central Plains. Extreme dryness also afflicted large portions of the eastern seaboard, particularly around the Carolinas.

[26] 2. Conditions were somewhat improved in 2003, but with extreme to severe drought conditions still covering between 10% to 25% of the United States. By July, drought had spread into the central and southern Great Plains with forest fires burning in Glacier National Park in Montana and in Arizona and Mexico.

[27] 3. The dry spell continued into 2004, but was alleviated in the west to some extent during the latter half of the year because of increased rainfall, although hydrologic drought persisted. For the first time since 1999, the area experiencing extreme to severe drought conditions dropped below 5% by the end of the year. NCDC ranked 2004 as the sixth wettest year on record for the contiguous United States.

4.2. Actual and Potential Evapotranspiration

[28] Figure 2 shows "monthly" (28-day) composites of clear-sky instantaneous latent heat flux from ALEXI at time t_2 (5.5 hours past local sunrise) for April–September of 2002–2004. Monthly composites of daytime total fluxes (including both clear and cloudy intervals) exhibit similar spatial characteristics. In general, the 3 years show consistent trends in the spatiotemporal evolution of ET over the United States. Early in the year, enhanced evapotranspiration (green tones) initiates in the southeast and then radiates up the eastern seaboard as forested regions begin to leaf out. By midyear, a strong gradient in ET is established east-west across the U.S, with a sharp discontinuity occurring midcontinent at the transition from dry to humid temperate climatic regimes. In the Midwest Corn Belt, green up is delayed until June–July when the dominant crops start to emerge, and the effects of crop senescence and harvest in that region become apparent by September.

[29] Despite these general similarities, significant interannual variability in spatial ET distributions does exist, driven primarily by differences in precipitation/climate and vegetation growth patterns. Physical interpretation of these ET maps (e.g., in terms underlying soil moisture conditions) must by necessity be constrained by local considerations. For instance, an area of elevated ET may or may not reflect recent precipitation depending on canopy cover conditions. In areas of very sparse vegetation, evaporation predominantly occurs from the soil surface layer—about the top 2–5 cm of the soil profile. Deeper layers are quickly disconnected from the system evaporative flux since the hydraulic conductivity rapidly drops to near zero as the surface skin dries out. High ET over areas of minimal vegetation cover is therefore an indicator of either very recent precipitation, or a very shallow water table. High ET rates will typically not be maintained over bare soil for long periods without additional replenishment of moisture content in the soil surface layer. Areas with thick, healthy vegetation cover, on the other hand, can maintain high ET for longer intervals after rain events because the roots provide access to moisture deeper within the soil profile.

[30] Normalization by the potential ET rate expected when soil moisture is nonlimiting serves to simplify interpretation of interannual ET variability, and to reduce some of this conditional dependency. Figure 3 shows 28-day composites of clear-sky f_{PET} ($\overline{f_{PET}}$) for June 2002–2004. These normalized fields are significantly smoother than are the actual ET fields for this month (Figure 2). The impact of the E-W vegetative gradient is reduced in $\overline{f_{PET}}$, improving comparability across climatic zones and highlighting areas impacted by stress. The Carolinas, for example, were experiencing extreme drought conditions in 2002.

[31] Note that the modified Priestley-Taylor (PT) approximation for PET used in ALEXI (Appendix B of A1) neglects advective forcings on evaporation rates, and may therefore underestimate PET in the more arid and semiarid

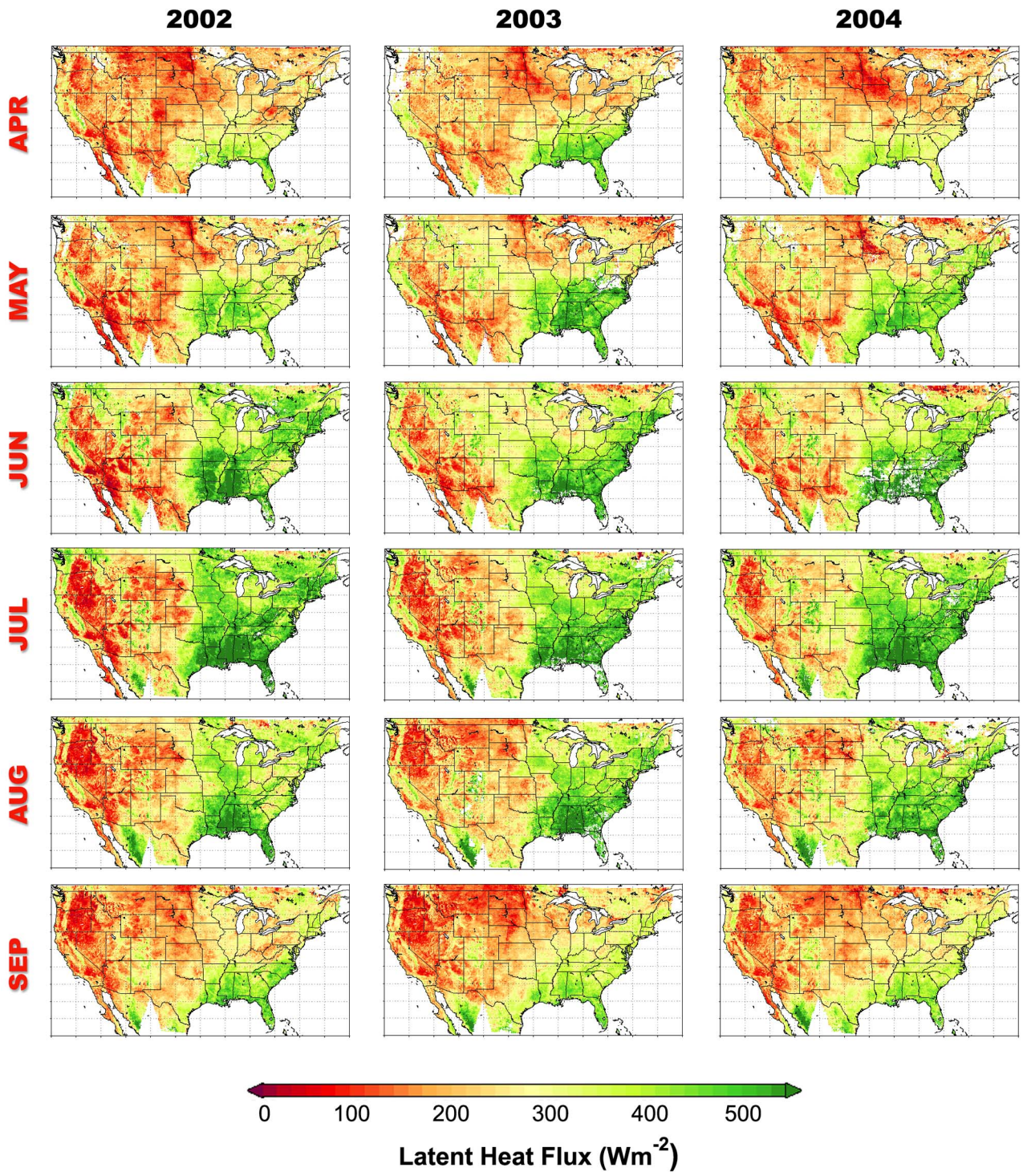

Figure 2. The 28-day clear-sky composites of instantaneous latent heat flux at time t_2 for April–September of 2002–2004.

climates of the western United States. Therefore actual $\overline{f_{PET}}$ values in the west may be somewhat lower than those displayed in Figure 3. The PT equation has been intentionally used in ALEXI instead of a Penman-Monteith approach to simplify input data requirements and to maintain compatibility with the PT equation used by the two-source land surface model as an initial estimate of the canopy transpiration rate. In future analyses, the PT coefficient could be made to vary with vapor pressure deficit to better capture aridity effects in the PET.

4.3. Interannual Variability in Evaporative Stress

[32] To further emphasize climatologically extreme events that have occurred during the period of investigation,

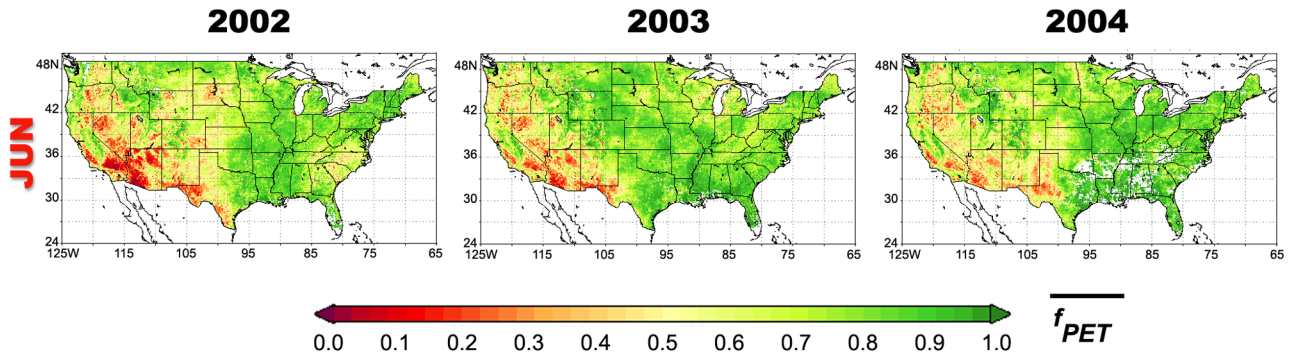

Figure 3. The 28-day clear-sky composites of f_{PET} for June of 2002–2004.

monthly deviations of $ESI = 1 - f_{PET}$ from 3-year average conditions ($\Delta\overline{ESI}$, equation (4)) are mapped in Figure 4. Red tones indicate areas characterized by above normal evaporative stress, while green areas are experiencing wetter than average conditions. The evaporative stress anomaly index $\Delta\overline{ESI}$ has the advantage, in comparison with ESI or f_{PET}, in that it is less sensitive to inaccuracies in the determination of PET. Effects of persistent spatiotemporal biases in estimated PET (e.g., because of neglect of atmospheric saturation deficit effects on the PT coefficient) are reduced by subtracting the climatological mean. Some features in Figure 4 are somewhat artificial, arising because only 3 years of data were used to establish the climatological basis (see, e.g., June, where an unusually wet area in the Great Plains in 2003 coincides with unusually dry area in 2004). These fields will improve as more years of archived model data become available to establish the baseline fluxes, smoothing the monthly climatological means.

4.4. Comparison With Other Drought Metrics

4.4.1. Palmer Z Index

[33] The spatiotemporal patterns in $\Delta\overline{ESI}$ shown in Figure 4 correlate well with trends in drought conditions observed across the United States over this 3-year interval, with increasingly wet (unstressed) conditions prevailing by mid 2004 as discussed in section 4.1. In Figure 4, the ALEXI evaporative stress anomaly index is compared with maps of the Palmer Z index, reflecting the departure from normal moisture conditions measured over the period 1900–2004 (data courtesy of the NCDC, http://www1.ncdc.noaa.gov/pub/data/cirs/). To improve comparability with the shorter-timescale ALEXI climatological record (2002–2004), anomalies in the Z index ($\Delta\overline{Z}$) with respect to monthly mean values for 2002–2004 have been displayed.

[34] Overall, there is good spatial correspondence between the ALEXI and Palmer Indices, which represent two completely independent means of detecting drought conditions. The Z index is based primarily on measurements of antecedent precipitation, while precipitation is not an input to the ALEXI model. In ALEXI, drought conditions are diagnosed from the remotely sensed LST and its relationship to the vegetation cover fraction.

[35] In April 2002, both $\Delta\overline{ESI}$ and $\Delta\overline{Z}$ highlight the dry conditions that prevailed in the southwest and extended into Colorado and the southern tip of Texas. ALEXI also picks up the drought that is beginning to develop along the East Coast. By June, the western drought had extended further north and east into the northern High Plains, as indicated by both ALEXI and Palmer indices. ALEXI also captures the extreme drought occurring in Virginia and the Carolinas, which led to forest fires, yield loss, and water shortages in these areas. Midsummer rains in North Carolina helped to downgrade drought severity in July 2002. However, the extended drought had already significantly impacted cotton and corn production in the Carolinas and Virginia. Lightning strikes in mid-July ignited the historic Biscuit Fire at the Oregon-California border, ultimately engulfing almost 500,000 acres. In August, both indices show incipient drought extending up the East Coast into New England and Maine, as confirmed by the Drought Monitor. The west remained engulfed in extreme drought through August 2002, but was relieved to some extent in September by above-average rainfall in New Mexico and Utah.

[36] In April 2003, both indices show central Texas to be extremely dry. These hot spots persist into May, while the southeast and central Plains are classified as wetter than average. In June, ALEXI indicates stress in Wisconsin and Michigan, also evident to a lesser extent in $\Delta\overline{Z}$. The Drought Monitor records the "introduction of abnormal dryness around Lake Michigan" at this time. Conditions in the central and southern Plains, including Texas improve in June 2003. In July, the southwest including Colorado was reclassified from wet or average to extremely dry conditions according to the Palmer Z index. The Drought Monitor reports that New Mexico had the driest July in the past 109 years. ALEXI also records this switch in moisture conditions. By August, dry conditions followed the border with Canada through the west and Midwest, reflected in both indices. ALEXI records a patch of stress in Missouri, Kansas, and Oklahoma that is not seen in the Z index but was noted in the Drought Monitor, which reported an increase of corn and soybean crops in poor to very poor condition this month in these states. The USDA reported 75% of Missouri's rangeland pasture to be in poor to very poor condition by the end of August 2003.

[37] In April 2004, a band of unusually dry conditions extended from California northward into Washington State and southeastward down into Florida, as seen in both $\Delta\overline{ESI}$ and $\Delta\overline{Z}$. The United States Drought Monitor for April reports that west Texas, New Mexico, and Colorado were wetter than usual because of heavy rains, which eased drought conditions in these areas, as is reflected in both indices. Monthly precipitation in the southwest was twice the climatological average, while in New Mexico, precipi-

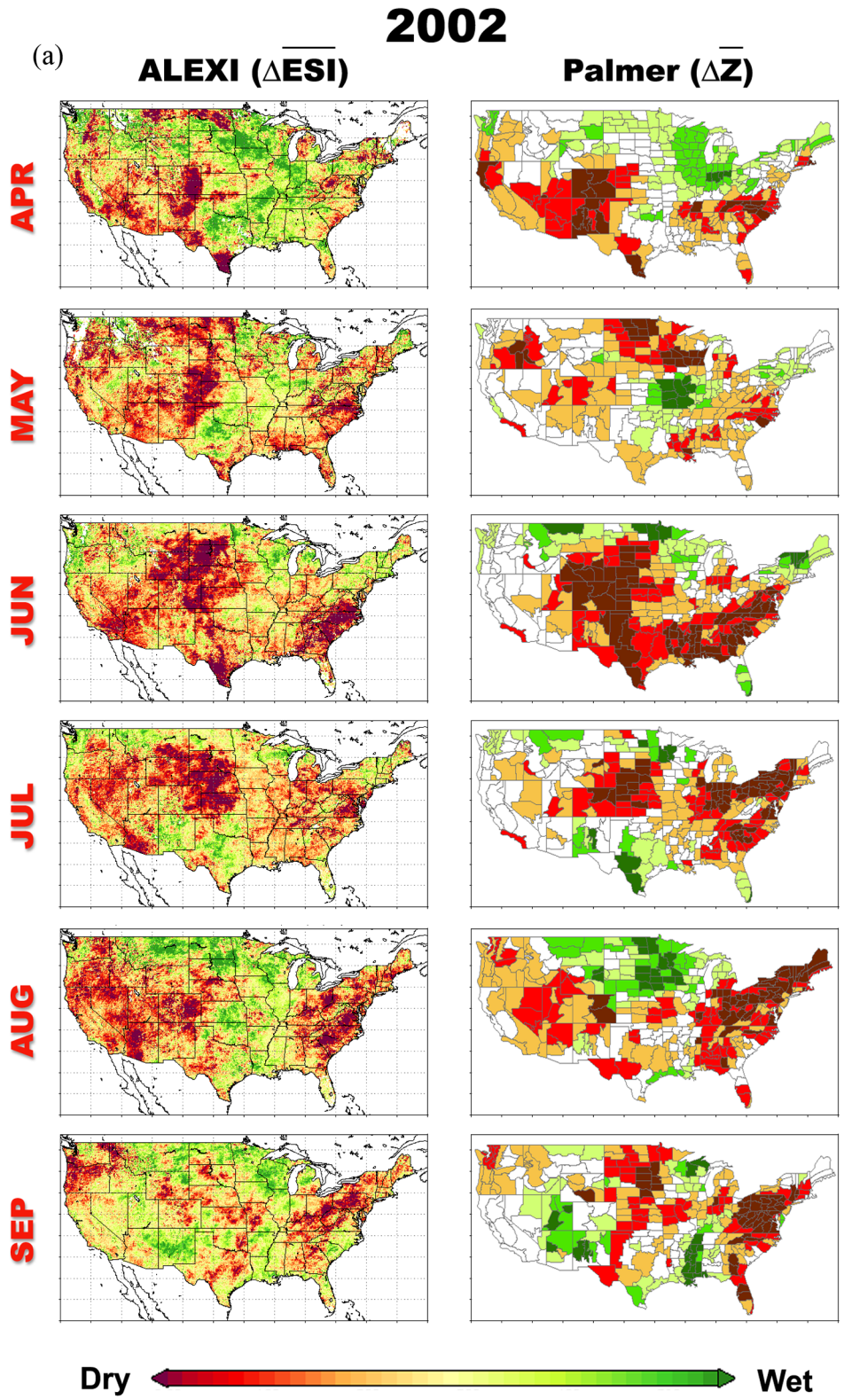

Figure 4. The 28-day clear-sky composites of the ALEXI evaporative stress anomaly index $\Delta\overline{ESI}$ compared with anomalies in the Palmer Z index ΔZ for April–September of (a) 2002, (b) 2003, and (c) 2004.

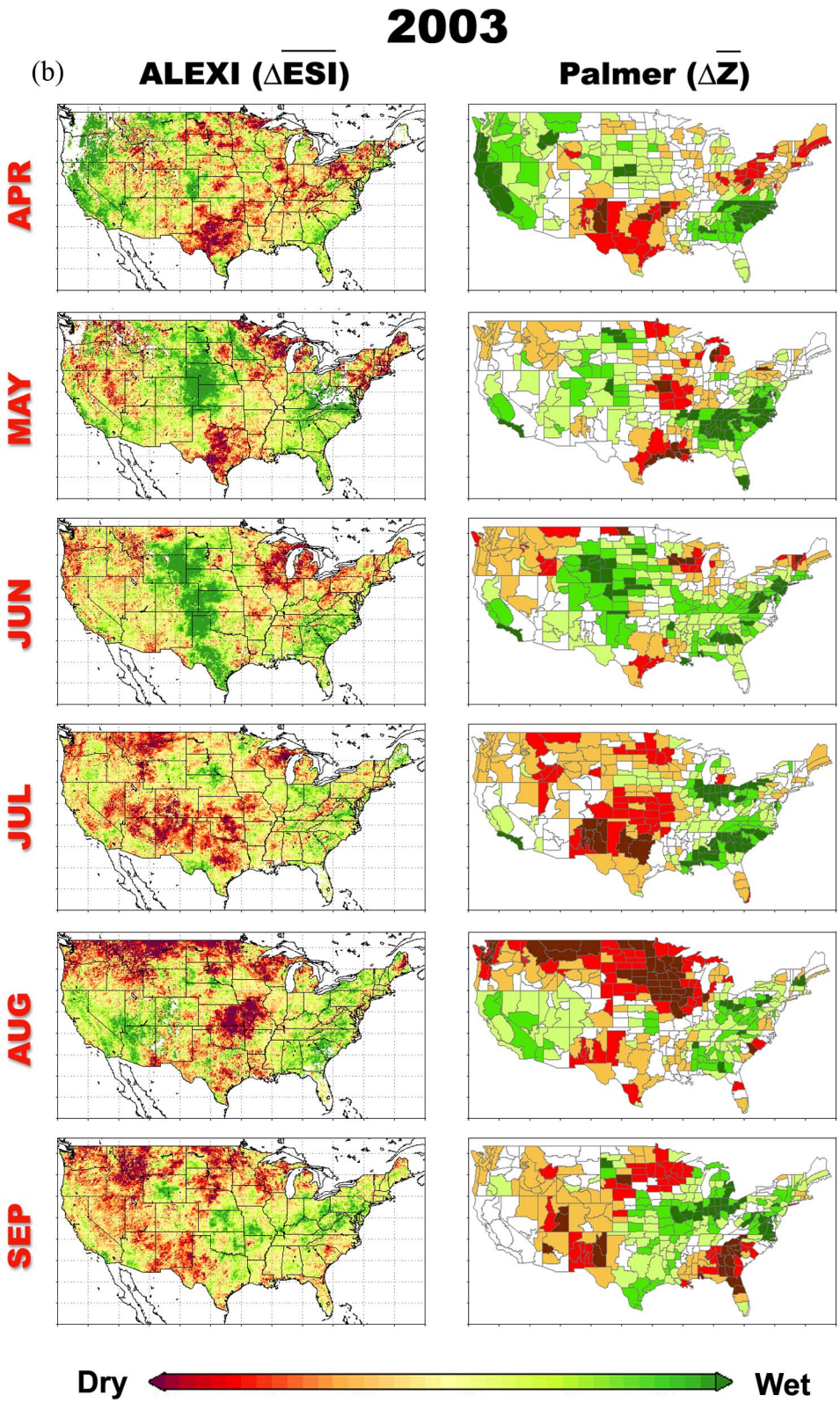

Figure 4. (continued)

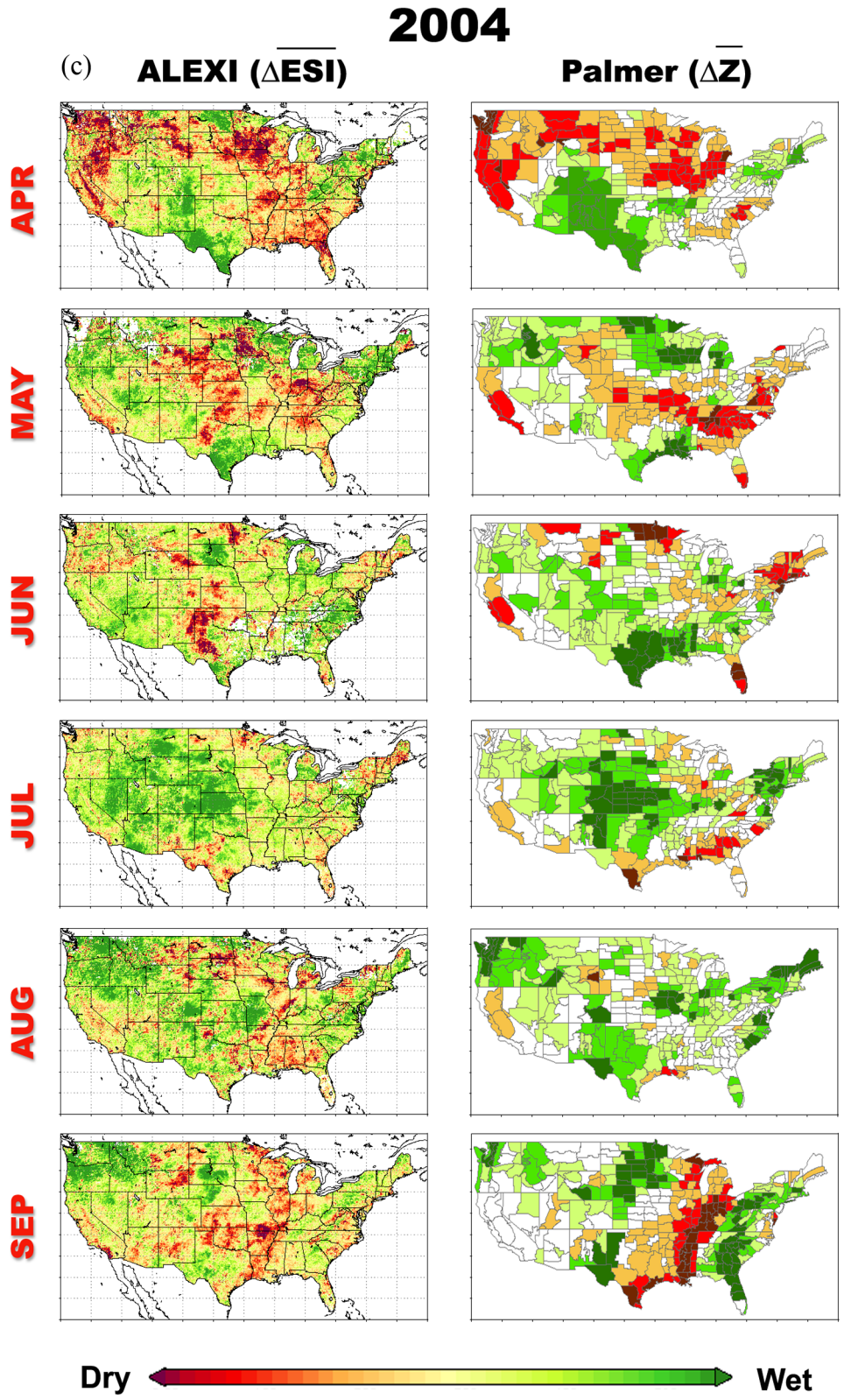

Figure 4. (continued)

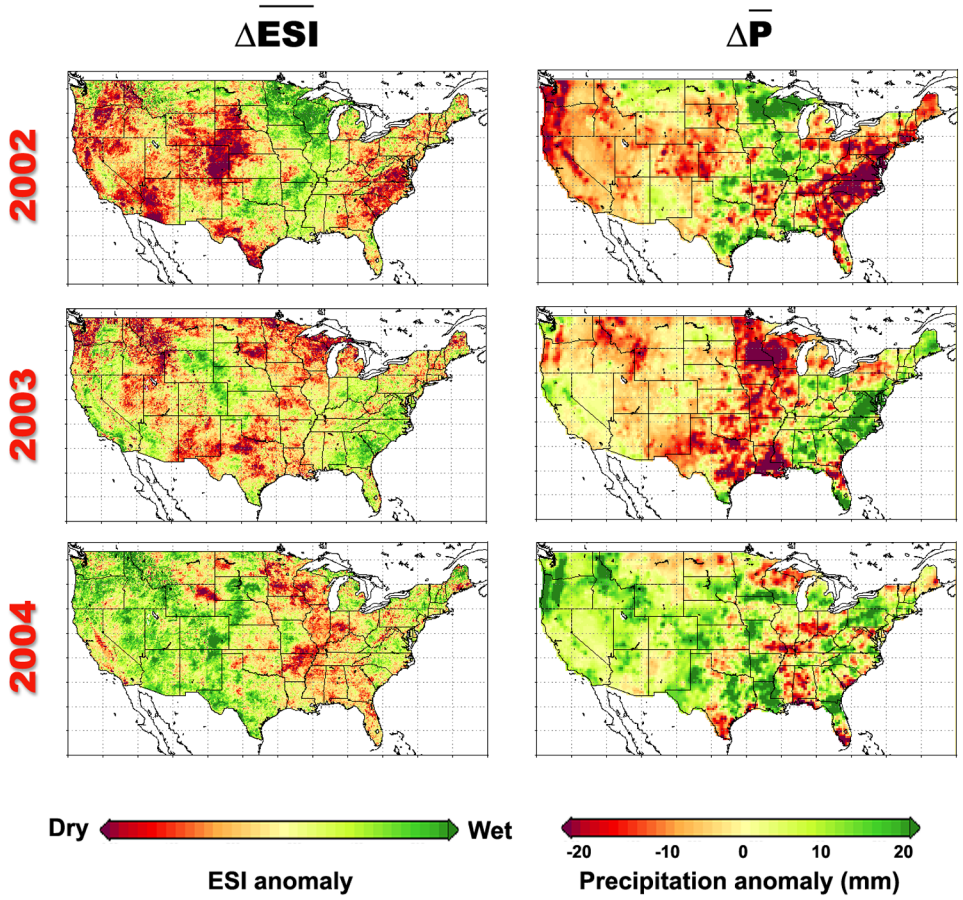

Figure 5. Fields of $\Delta\overline{ESI}$ and $\Delta\overline{P}$ for 2002–2004, averaged over April–September.

tation increased fourfold. In May, the southern and central Plains suffered from lack of rain. Unlike the Z index, ALEXI indicates stress in southwest Minnesota, while the Drought Monitor also reported moderate to severe drought in this area. In June 2004, the 28-day ALEXI composite picks up signatures of drought in the Texas panhandle, Oklahoma and Kansas that extended from May into the early parts of June. The Z index resets at the first of the month, and therefore is not influenced by conditions in May. In July 2004, ALEXI and $\Delta\overline{Z}$ show much of the west and central United States as wetter than average for the 3-year period of record. These wet conditions persist into the month of August. In September, dry conditions prevailed in a N–S band from Wisconsin and Michigan down to Louisiana (see both $\Delta\overline{ESI}$ and $\Delta\overline{Z}$). Precipitation records show that little or no rain occurred over southern Missouri and Arkansas in 2004 during September, and Arkansas experienced its third-driest September on record.

[38] In general, there is good qualitative agreement between spatial patterns in $\Delta\overline{ESI}$ and $\Delta\overline{Z}$, indicating a detectable impact of antecedent precipitation (as interpreted by the Palmer index) on land surface temperature at continental scales. The ALEXI evaporative stress anomaly index shows persistence in coherent spatial features from month to month, reflecting a natural time integration of moderate-term moisture conditions insofar as they affect LST and evaporative fluxes. Features in the Z index disappear abruptly at the end of the month given the imposed time constant of integration. Given its basis in remote sensing, ALEXI is able to provide stress information at significantly higher resolution than is the Palmer index.

4.4.2. Precipitation

[39] Maps of $\Delta\overline{ESI}$ and precipitation anomalies, $\Delta\overline{P}$, with both quantities averaged over the months of April–September, are displayed in Figure 5 for 2002–2004—maps of anomalies in ET show similar patterns. While the spatial correspondence is good, we do not necessarily expect perfect agreement between these fields. The timing of precipitation events with respect to the vegetation growth cycle and antecedent moisture status will influence their impact on system ET. When there is little green vegetation present, or if the soil profile is already near its water-holding capacity, the time-integrated impact of a large rainfall on evapotranspiration will be lessened. Similarly, a large rainfall deficit in the eastern United States in 2002 results in a somewhat weaker stress signal than does a smaller deficit in Colorado, Kansas and Nebraska where the cover fraction is lower and the active component of soil moisture is depleted with a shorter time constant.

[40] The good agreement between these fields indicates that the surface temperature signature, as interpreted by the two-source land surface model in ALEXI, is indeed giving useful information about soil moisture conditions. Because of the influence of moisture stress on canopy temperature,

these thermal-based methods even show sensitivity to moisture content in the eastern United States under high vegetation cover and therefore may be a valuable complement to microwave soil moisture retrieval techniques, which lose sensitivity under these conditions.

5. Conclusions and Future Research

[41] The surface energy balance modeling techniques described in this paper have demonstrated skill in identifying areas subject to soil moisture stress primarily on the basis of remotely sensed surface temperature and vegetation index data. A satellite-derived evaporative stress index, given by 1 minus the ratio of actual to potential ET ($ESI = 1 - f_{PET}$), highlights areas where ET has been suppressed because of depleted soil moisture or some other stressor. Simpler TIR/VI-based drought indices like the vegetation health index do not account for important forcings on surface temperature, such as available energy and atmospheric conditions, and can therefore generate spurious drought detections under certain circumstances. Surface energy balance inherently incorporates these forcings, constraining ET response in both energy and water-limited situations.

[42] Examining monthly clear-sky composites of *ESI* for April–October 2002–2004, the ALEXI stress index shows good spatial correlation with the Palmer Z index, which is based on monthly deviations in precipitation from climatic norms. The *ESI* also compares well directly to anomalies in monthly precipitation fields. Unlike the standard meteorologically based drought indicators, the ALEXI algorithm does not use precipitation and soil texture data as input – fields that are difficult to specify accurately at high resolution across continental scales. The spatial resolution of the ALEXI *ESI* is limited by the resolution of the available geostationary thermal data, typically 5–10 km; drought-affected areas can therefore be identified at the subcounty level. An associated flux disaggregation technique, DisALEXI [*Norman et al.*, 2003; *Anderson et al.*, 2004, 2005], using TIR and VI data from polar orbiting systems such as Landsat or Moderate Resolution Imaging Spectroradiometer (MODIS), facilitates stress mapping at even finer resolutions (60 m to 1 km).

[43] The ALEXI system has been fully automated and can function with limited ground-based inputs, and therefore is eminently portable to other continents with geostationary satellite coverage. Preliminary flux evaluations have been conducted over Spain using thermal data from Meteosat with minimal modifications required to the model infrastructure. Because the two-source land surface component of ALEXI partitions ET into canopy transpiration and soil evaporation components, we can potentially probe moisture conditions both in the soil surface layer and the root zone. The surface layer is expected to respond more rapidly to precipitation deficits, and therefore the ability to separate these two moisture pools is an advantage of the two-source approach in ALEXI in comparison with single-source thermal land surface models (A1). Ongoing studies are examining the utility of ESI_S and ESI_C for monitoring both meteorological and agricultural drought, respectively, within this unified modeling framework.

[44] Satellite-derived drought indices have a disadvantage in terms of temporal ''extendability'' [*Keyantash and Dracup*, 2002]; the long-term climatological record for the *ESI* is limited by the time span of the geostationary satellite record. A1 demonstrate that noise in f_{PET} is uneven across the monitoring domain because of variability in cloud cover persistence, and incomplete cloud clearing of the thermal satellite inputs can add spurious artifacts to the product. Improved methods for cloud masking should increase the robustness of shorter-term (e.g., weekly) *ESI* composites. Future work will investigate the impact of alternative forms for computing potential ET on drought severity predictions, e.g., imposing a crop coefficient or VPD-dependent Priestley-Taylor coefficient. While it is likely that PET is underestimated in the western United States by employing the Priestley-Taylor formulation, some of this bias is removed in the computation of temporal deviations from mean conditions. Further validation of actual ET estimates from ALEXI in southwestern field sites is underway, testing model response to variable VPD and advective conditions. Good agreement has been found between flux estimates from the two-source land surface component of ALEXI and flux measurements made in southern Arizona under a range in surface moisture conditions [*Li et al.*, 2007].

[45] *Svoboda et al.* [2002] describe recent efforts to objectively blend multiple indices to create a drought product that is less subjective and labor intensive than the manually generated Drought Monitor. Ground- and satellite-based indicators provide independent information regarding surface moisture conditions, and in combination should improve regional drought assessments if errors are uncorrelated. With ALEXI/DisALEXI, a multiscale monitoring approach is possible. Composites of the ALEXI *ESI* can be generated weekly using geostationary satellite data, identifying areas at the continental scale that appear to be experiencing moisture stress. These areas can then be targeted for disaggregation using high-resolution imagery from polar orbiting satellites. Landsat-resolution ($\sim$100 m) thermal data typically resolves individual fields, facilitating subcounty level assessments of vegetation health by crop type. Given the demonstrated utility of the thermal band for remote drought detection, there is clear necessity for maintaining a comprehensive and continuous record of high-quality TIR imagery covering the globe at a variety of spatial resolutions.

[46] **Acknowledgments.** This work was supported by the NASA EOS and Land Surface Hydrology Programs. In particular, funding for this research was provided primarily by NASA grant NAG13-99008 and in part by USDA Cooperative Agreement 58-1265-1-043.

References

Allen, R. G., M. Tasumi, A. T. Morse, and R. Trezza (2005), A Landsat-based energy balance and evapotranspiration model in western U.S. water rights regulation and planning, *J. Irrig. Drain. Syst.*, *19*, 251–268.

Alley, W. M. (1984), The Palmer drought severity index: Limitations and assumptions, *J. Clim. Appl. Meteorol.*, *23*, 1100–1109.

Anderson, M. C., J. M. Norman, G. R. Diak, W. P. Kustas, and J. R. Mecikalski (1997), A two-source time-integrated model for estimating surface fluxes using thermal infrared remote sensing, *Remote Sens. Environ.*, *60*, 195–216.

Anderson, M. C., J. M. Norman, J. R. Mecikalski, R. D. Torn, W. P. Kustas, and J. B. Basara (2004), A multi-scale remote sensing model for disaggregating regional fluxes to micrometeorological scales, *J. Hydrometeorol.*, *5*, 343–363.

Anderson, M. C., J. M. Norman, W. P. Kustas, F. Li, J. H. Prueger, and J. M. Mecikalski (2005), Effects of vegetation clumping on two-source model estimates of surface energy fluxes from an agricultural landscape during SMACEX, *J. Hydrometeorol.*, *6*, 892–909.

Anderson, M. C., J. M. Norman, J. R. Mecikalski, J. P. Otkin, and W. P. Kustas (2007), A climatological study of evapotranspiration and moisture stress across the continental United States based on thermal remote sensing: 1. Model formulation, *J. Geophys. Res.*, doi:10.1029/2006JD007506, in press.

Bastiaanssen, W. G. M., E. J. M. Noordman, H. Pelgrum, G. Davids, B. P. Thoreson, and R. G. Allen (2005), SEBAL model with remotely sensed data to improve water-resources management under actual field conditions, *J. Irrig. Drain. Eng.*, *131*, 85–93.

Bayarjargal, Y., A. Karnieli, M. Bayasgalan, S. Khudulmur, C. Gandush, and C. J. Tucker (2006), A comparative study of NOAA-AVHRR derived drought indices using change vector analysis, *Remote Sens. Environ.*, *105*, 9–22.

Dracup, J. A., K. S. Lee, and E. G. Paulson Jr. (1980), On the definition of droughts, *Water Resources Res.*, *16*, 297–302.

Guttman, N. B. (1997), Comparing the Palmer drought index and the standardized precipitation index, *J. Am. Water Resour. Assoc.*, *35*, 113–121.

Guttman, N. B., J. R. Wallis, and J. R. M. Hosking (1992), Spatial comparability of the Palmer drought severity index, *Water Resour. Bull.*, *28*, 1111–1119.

Heim, R. R. (2002), A review of twentieth-century drought indices used in the United States, *Bull. Am. Meteorol. Soc.*, *83*, 1149–1165.

Idso, S. B., R. D. Jackson, P. J. Pinter, R. J. Reginato, and J. L. Hatfield (1981), Normalizing the stress-degree-day parameter for environmental variability, *Agric. Meteorol.*, *24*, 45–55.

Jackson, R. D., S. B. Idso, R. J. Reginato, and P. J. Pinter (1981), Canopy temperature as a crop stress indicator, *Water Resour. Res.*, *17*, 1133–1138.

Karl, T. R. (1983), Some spatial characteristics of drought duration in the United States, *J. Clim. Appl. Meteorol.*, *22*, 1356–1366.

Karl, T. R. (1986), The sensitivity of the Palmer drought severity index and Palmer's Z-index to their calibration coefficients including potential evapotranspiration, *J. Clim. Appl. Meteorol.*, *25*, 77–86.

Karnieli, A., M. Bayasgalan, Y. Bayarjargal, N. Agam, S. Khudulmur, and C. J. Tucker (2006), Comments on the use of the vegetation health index over Mongolia, *Int. J. Remote Sens.*, *27*, 2017–2024.

Keyantash, J., and J. A. Dracup (2002), The quantification of drought: An evaluation of drought indices, *Bull. Am. Meteorol. Soc.*, *83*, 1167–1180.

Kogan, F. N. (1997), Global drought watch from space, *Bull. Am. Meteorol. Soc.*, *78*, 621–636.

Li, F., W. P. Kustas, M. C. Anderson, J. H. Prueger, and R. L. Scott (2007), Effect of remote sensing spatial resolution on interpreting tower-based flux observations, *Remote Sens. Environ*, in press.

Mecikalski, J. M., G. R. Diak, M. C. Anderson, and J. M. Norman (1999), Estimating fluxes on continental scales using remotely-sensed data in an atmosphere-land exchange model, *J. Appl. Meteorol.*, *38*, 1352–1369.

Monteith, J. L. (1965), Evaporation and environment, in *The State and Movement of Water in Living Organisms*, *Symp. Soc. Exp. Biol.*, vol. 19, pp. 205–234, Cambridge Univ. Press, New York.

Moran, M. S. (2003), Thermal infrared measurement as an indicator of plant ecosystem health, in *Thermal Remote Sensing in Land Surface Processes*, edited by D. A. Quattrochi and J. Luvall, pp. 257–282, Taylor and Francis, Philadelphia, Pa.

Moran, M. S., T. R. Clarke, Y. Inoue, and A. Vidal (1994), Estimating crop water deficit using the relation between surface-air temperature and spectral vegetation index, *Remote Sens. Environ.*, *49*, 246–263.

Myneni, R. B., et al. (2002), Global products of vegetation leaf area and fraction absorbed PAR from year one of MODIS data, *Remote Sens. Environ.*, *83*, 214–231.

Norman, J. M., M. C. Anderson, W. P. Kustas, A. N. French, J. Mecikalski, R. Torn, G. R. Diak, T. J. Schmugge, and B. C. W. Tanner (2003), Remote sensing of surface energy fluxes at 10^1-m pixel resolutions, *Water Resour. Res.*, *39*(8), 1221, doi:10.1029/2002WR001775.

Otkin, J. A., M. C. Anderson, J. R. Mecikalski, and G. R. Diak (2005), Validation of GOES-based insolation estimates using data from the United States Climate Reference Network, *J. Hydrometeorol.*, *6*, 460–475.

Palmer, W. C. (1965), Meteorological drought, 58 pp, *U.S. Weather Bur. Res. Pap. 45*, NOAA, Silver Spring, Md.

Palmer, W. C. (1968), Keeping track of crop moisture conditions, nationwide: The new crop moisture index, *Weatherwise*, *21*, 156–161.

Svoboda, M., et al. (2002), The drought monitor, *Bull. Am. Meteorol. Soc.*, *83*, 1181–1190.

Tasumi, M., R. Trezza, R. G. Allen, and J. L. Wright (2005), Operational aspects of satellite-based energy balance models for irrigated crops in the semi-arid U. S., *J. Irrig. Drain. Syst.*, *19*, 355–376.

Wilhite, D. A., and M. H. Glantz (1985), Understanding the drought phenomenon: The role of definitions, *Water Int.*, *10*, 111–120.

M. C. Anderson and W. P. Kustas, Hydrology and Remote Sensing Laboratory, ARS, USDA, Bldg 007 Rm 104 BARC-West, 10300 Baltimore Ave, Beltsville, MD 20705, USA. (manderson@hydrolab.arsusda.gov; bkustas@hydrolab.arsusda.gov)

J. R. Mecikalski, National Space Science and Technology Center, University of Alabama in Huntsville, 320 Sparkman Drive, Huntsville, AL 35805, USA. (johnm@nsstc.uah.edu)

J. M. Norman, Department of Soil Science, University of Wisconsin-Madison, 263 Soils, 1525 Observatory Drive, Madison, WI 53706, USA. (jmnorman@facstaff.wisc.edu)

J. A. Otkin, Cooperative Institute for Meteorological Satellite Studies, University of Wisconsin-Madison, 1225 West Dayton Street, Madison, WI 53706, USA. (jason.otkin@ssec.wisc.edu)